Journal of Optoelectronic and Biomedical Materials Vol. 16, No. 4, October-December 2024, p. 199-209

The optical and electrochemical characteristics of silver nanoparticles, besides antibacterial and antifungal properties using crocus sativus.l petal

A. C. Preethi, V. Hariharakrishnan, V. Saraswathi *
PG and Research Department of Physics, National College (Autonomous), Affiliated to Bharathidasan University, Tiruchirappalli, Tamil Nadu, India

The manufacture of silver nanoparticles using plant extract is a simple, worthwhile, and ecologically friendly method. We present the use of in this study Crocus sativus .L petal extract is being used to create environmentally friendly nanoparticles. In the green approach, UV-Vis spectroscopy is utilised to characterise and confirm the presence of silver nanoparticles containing reduced silver ions. The XRD confirms the silver nanoparticles' crystalline structure formed in this process. Scanning electron microscopy reveals predominantly spherical and triangular shapes of the nanoparticles, with sizes ranging from 20 to 45 nm. To examine electrochemical properties, cyclic voltammetry and electrochemical impedance studies were utilised. Consequently, when subjected to the disc diffusion method, the synthesized silver nanoparticles exhibit enhanced antibacterial activity against various strains such as Pseudomonas aeruginosa, Proteus vulgaris, Enterococcus faecalis, Streptococcus Mutans, Enterococcus aeruginosa, and Bacillus subtilis.

(Received December 16, 2023; Accepted December 10, 2024)

Keywords: Crocus sativus.L, Silver nanoparticles, UV-Vis, XRD, SEM and antimicrobial activity

1. Introduction

Noble metal nanoparticles have lately piqued the interest of academics due to their distinct mechanical, optical, magnetic, chemical, and electrical capabilities that set them apart from bulk materials. Co precipitation, sol-gel synthesis, sonochemical synthesis, inert gas condensation, template synthesis, ion sputtering scattering, spark discharge, micro emulsion, biological synthesis, microwave synthesis, and hydrothermal synthesis are only a few of the various ways for creating nanoparticles. (Figure-1). These peculiar and distinguishing characteristics may be attributable to their extremely small diameters and massive surface areas. Because of these qualities, metallic nanoparticles are used in a variety of applications [1]. Because of the vast variety of unique features and uses, the process of manufacturing silver nanoparticles has gained a lot of interest that Ag NPs possess, such as surface-enhanced Raman scattering, electrical conductivity, catalysis, antimicrobial and antibacterial activities, magnetic and optical polarizability, and antimicrobial activities [2, 3]. NPs have been created using electrochemistry, photochemistry, chemical reduction, and physical methods such as physical vapour condensation.

* Corresponding author: saraswathiv@nct.ac.in
https://doi.org/10.15251/JOBM.2024.164.199

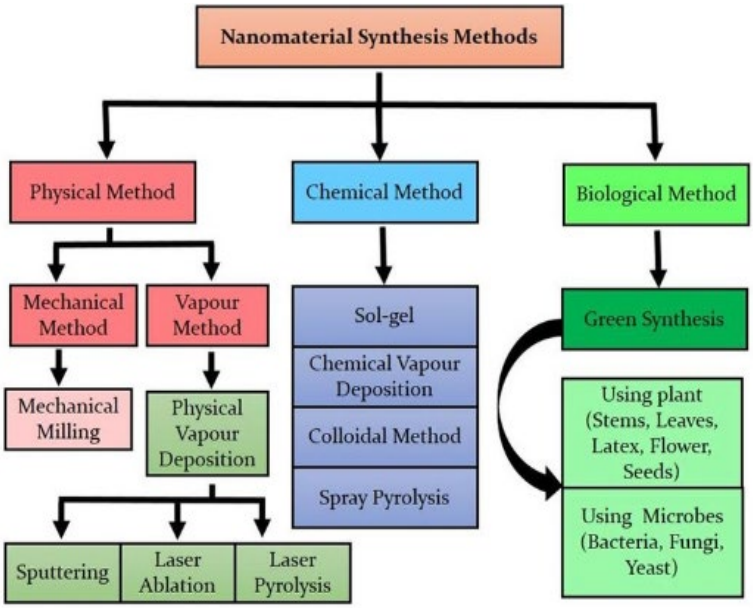

Fig. 1. Methods of synthesis nanoparticles.

In nanomaterials science, green synthesis is increasingly being used to create NPs. In what is known as "green synthesis," metal salts are mixed with organic components such as vitamins, carbohydrates, microbes, plant extracts, and biodegradable polymers to generate nanoparticles (Figure-2). Green synthesis is favoured over chemical and physical processes because it is less expensive, better for the environment, and easier to scale up for large-scale synthesis. It also removes the need for dangerous chemicals, as well as high pressure, energy, and temperature. A critical stage in the ecologically friendly production of AgNPs is the chemical reduction of AgNO3 using plant extract. This study describes a green method for producing silver nanoparticles that uses saffron plant extract as a potential bio source for stabilising and reducing agents [4]. Saffron is scientifically known as Crocus sativus L. It is a member of the iris family. Saffron is a valuable plant that is often referred to as “Red Gold.” This plant is used to make a variety of foods, clothing, and medications.

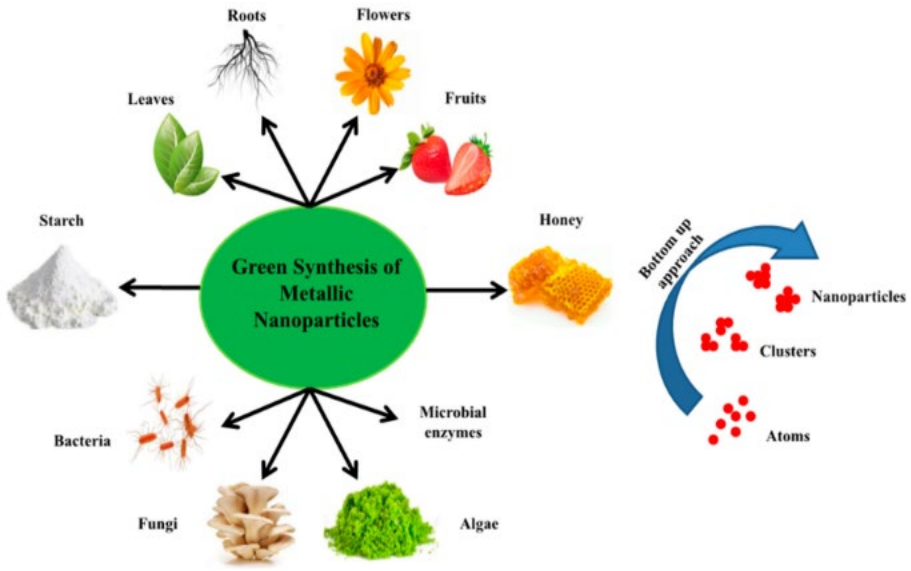

Fig. 2. Metallic nanoparticles synthesised in an environmentally friendly manner.

Silver is a non-toxic inorganic antibacterial substance that may kill over 650 different harmful bacteria species. Despite a lack of comprehensive biological and toxicological data, AgNPs are becoming more common in both everyday life and medicine. Around the world, AgNPs are being employed in a broader range of commercial products. Nanoparticles are consumed by living creatures either actively or passively, generating worries about their toxicity. As a result, it is critical to set the conditions for the proper usage of nanoparticles in order to achieve certain biological goals. The effects of AgNPs on the environment, animals, and humans are unknown, as are any potential concerns about their possibly harmful short- and long-term deleterious consequences. Nonetheless, there is a lack of clear understanding in these domains. In addition, AgNPs are employed in wastewater treatment and the garment sector. Silver is employed in metal nanoparticles due of its antibacterial and therapeutic properties. Topical ointments containing silver and silver nanoparticles are commonly used to treat burns and open wounds and to prevent infection. Antibiotics and polymers contaminated with silver were used to create medical implants and gadgets. The antibacterial activity of silver nanoparticles is most strongly influenced by their size. Smaller nanoparticles have more surface area, which increases chemical stability and antibacterial activity [5].

2. Materials and methods

2.1. The extraction of a leaf:

The grocery store sold fresh Crocus sativus L. petals. Before filtering, 10g of petals were finely chopped and steeped in 150 mL of de-ionized water for 24 hours at 65ºC.

2.2. Biosynthesis of Ag Nanoparticles:

After dissolving 0.509g of AgNO3 (0.1M) in 30ml of distilled water, the mixture was agitated for an hour. The petal extract was then added in 75 ml increments to the swirling AgNO3 solution. The material was vigorously mixed. After two hours, the bright red fades to dark brown. The solution was to keep it at 120°C for four hours in a hot air oven. The sample was then heated for 10 minutes at 250°C in a muffle furnace. After then, the sample was pulverised. The nanoparticles were stored in a dark room for future studies.

3. Characterization of AgNPs

Characterization of synthesised silver nanoparticles was accomplished using UV-Vis spectroscopy, X-ray diffractometry, and Scanning electron microscopy.

4. Electrochemical studies

To evaluate the electro catalytic and charge transfer properties of synthesised nanoparticles, electrochemical techniques such as cyclic voltammetry and impedance spectroscopy are used.

5. Results and discussion

5.1. UV-visible spectroscopy

The creation of silver nanoparticles was validated by measuring their absorbance using UV-Vis spectroscopy, as silver nanoparticles had the highest absorbance in the UV region. The wavelength range for measuring absorbance is 200 nm to 700 nm. Silver nanoparticles have a high absorption and scattering efficiency. Because conduction electrons on the metal surface experience a collective oscillation when energised by light at particular wavelengths, they have a high interaction with light.

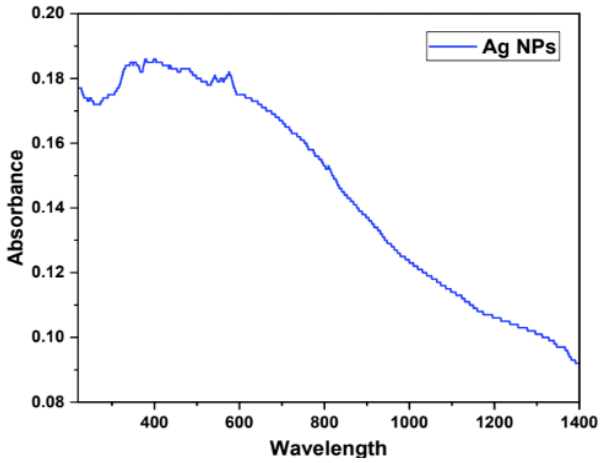

Fig. 3. UV-Visible analysis of silver nanoparticles.

Fig. 3. Depicts the UV absorption spectra of the silver nanoparticle solution, which shows an absorption peak in the visible range of 354.5 nm. The graph reveals a prominent absorption peak for the sample silver nanoparticles. Because silver nanoparticles have a large absorption peak due to surface plasmon excitation in the UV region, the absorption spectra obtained by UV-Vis spectroscopy are accurate in demonstrating their existence [6].

5.2. XRD

Crystallinity, isomorphous substitution, particle size, and molecular and crystal structures can all be determined by XRD. It can also distinguish between drugs and detect active components. The many diffraction peaks formed when X-ray radiation reflects on any particle reveal the crystalline lattice's physicochemical features. XRD may be used to explore the structural characteristics of a wide range of materials, including superconductors, glasses, biomolecules, inorganic catalysts, and polymers. The layout is critical for determining the diffraction peak parameters. By comparing the diffracted beams to the JCPDS reference details, the specific diffraction light source of each material may be recognised. Bragg's law is used by XRD.

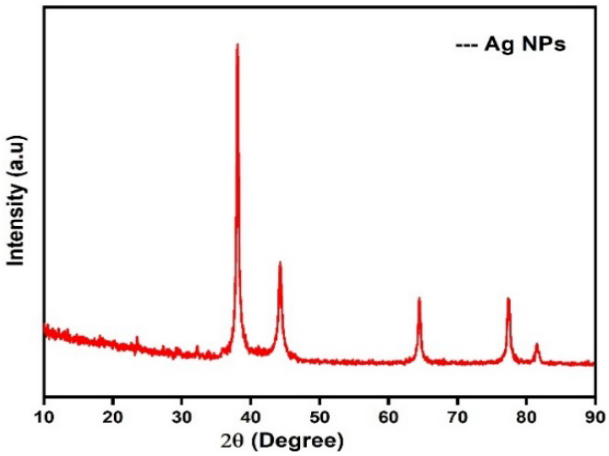

Fig. 4. The X-Ray Diffraction pattern of silver nanoparticles.

The size of AgNPs was calculated using the Debye-Scherer formula.

$$D=K\lambda/\beta\cos\theta$$

where D is the crystalline size, K is the Scherer constant, λ is the wave length of the utilised X-ray beam (1.54, 184), and β is the peak's FWHM, θ and is the Bragg angle. The size, phase identification, and crystallinity of the AgNPs were determined by XRD analysis. Silver's Bragg reflection planes 111, 200, 220, 311, and 222 correspond to five unique, steep peaks at 38.08°, 44.09°, 64.42°, 77.37°, and 82.52°, respectively (Figure-4) [6]. The XRD pattern clearly demonstrated that the AgNPs formed by the reduction of Ag^{+} ions in aqueous extract of saffron waste were crystalline. The signal in the (111) plane is stronger than in the other planes, indicating that silver nanoparticles have grown preferentially in that direction [7, 8].

5.3. Scanning electron microscope

Surface imaging techniques such as scanning electron microscopy (SEM) may distinguish between distinct particle sizes, particle dispersion, nanoparticle topologies, and the surface appearance of Ag NPs at both the micro and nanoscales. By manually counting and calculating the particles or using the appropriate tools, we may examine the form of the nanoparticles and generate a histogram from the SEM pictures. The components and structure of silver nanoparticles were studied. The morphological features of silver nanoparticles produced from Crocus sativus L extract depicts a SEM image (Figure-5). The dimensions of the triangular and spherical forms in this image range from 20 to 45 nm. This SEM image clearly shows the aggregation of silver nanoparticles.

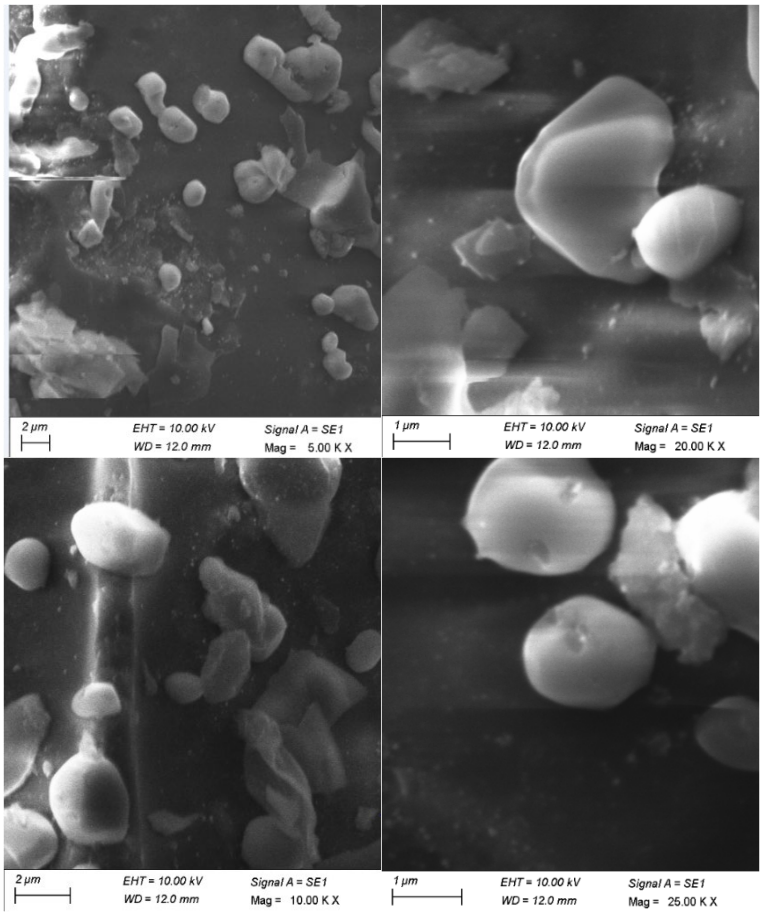

Fig. 5. SEM image for Ag NPs synthesised by the extract of Crocus sativus .L at various exaggeration.

5.4. Electrochemical analysis

5.4.1. Cyclic voltammetry analysis

The electro catalytic activity of biosynthesized AgNPs was measured using cyclic voltammetry. Cyclic voltammetry tests on AgNPs synthesised with saffron extract as the reductant and stabilising agent were done to assess whether AgNPs were present in the samples prepared using the green chemistry technique. In cyclic voltammetry testing, a glassy carbon electrode (GC) was utilised as the working electrode, a platinum electrode as the counter-electrode, and a saturated calomel electrode (SCE) as the reference electrode.

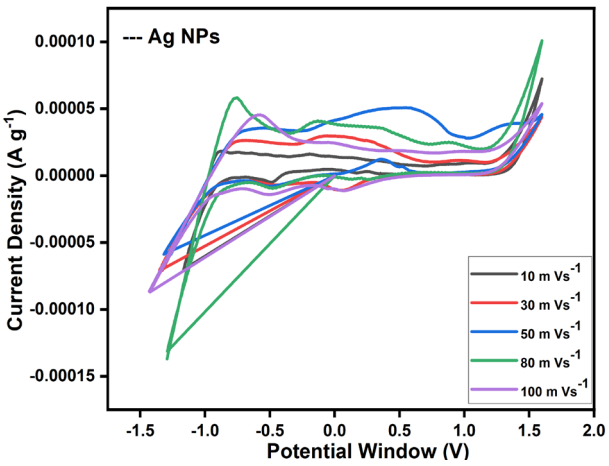

Fig. 6. Cyclic voltammetry studies of silver nanoparticle.

The GC electrode was altered by spraying varied volumes of silver nanoparticles spray over the surface and allowing it to dry at room temperature. The peak current of the oxidation process, like that of surface stripping, is proportional to the scan rate. The electrolyte solution was measured between -1.0 V and +1.5 V in a potential window with scan rates of 10, 30, 50, 80, and 100 mV/s. The anodic peak currents in silver nanoparticles increased from 10 to 100 mVs-1 as the scan rate increased (Figure-6). Oxygen-containing functional groups cause the CV curve's peak at 0.1 V (Figure-6). The order in which the chemicals are introduced throughout the manufacturing process has no effect on the electrochemical activity of AgNPs. The most stable silver nanoparticles have been discovered to be those produced after a reductant is added.

5.4.2. Impedance analysis

When an alternating current (AC) current is present, an AC field is created across the Sodium sulphate electrolyte by alternately charging the two electrodes with positive and negative polarity. As a result of the supplied voltage, the ions begin to oscillate in time. In these impedance graphs (Figure-7), the capacitor Zi reflects the polarity of the stationary polymer chains, while the resistor Zr depicts the flow of ions. It can be observed that the impedance plots exhibit an inclined straight line in the low frequency band as salt concentrations increase, which is explained by electrode polarisation. The ions at each electrode alternately assemble and deplete as they move across the alternating field.

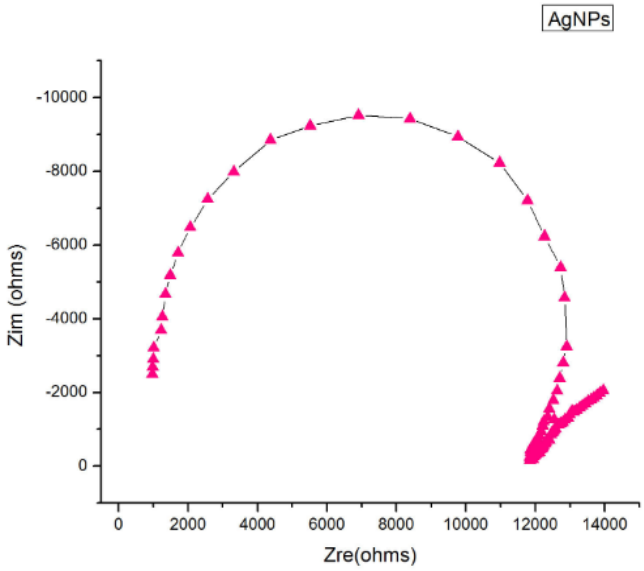

Fig. 7. Impedance analysis of silver nanoparticles.

On each half-cycle, ionic charges are observed to build up in the electrolyte close to the electrodes. These charges on the electrodes are balanced by electrical charges that are equal and in opposition to one another. This polarisation process is known as electrode polarisation, or EP. With an increase in salt content, the EP area visibly grows. It was discovered that the centres of each semicircle were smaller than the actual axes, indicating that the linked relaxation processes are not of the Debye type.

Impedance spectroscopy and equivalent circuit analyses reveal higher electrochemical activity in Ag catalyst. This increase in capacitance can be due to the as-grown Ag's tiny particle size and lack of aggregation, which promotes robust redox reaction activity.

6. Antimicrobial activities

6.1. Collection of test pathogens

As test organisms for the antifungal activity, Candida vulgaris (MTCC 6380) and Aspergillus flavus (MTCC 9643) were generated for the investigation. Pseudomonas aeruginosa (MTCC 1688), Proteus vulgaris (MTCC 6380), Enterococcus faecalis (MTCC 29213), Streptococcus mutans (MTCC 25175), Bacillus subtilis (MTCC 5981), and Enterococcus aeruginosa (MTCC 27853) were among the microorganisms that the samples were active against.

6.2. Antibacterial activity measurement using the disc diffusion method

The disc diffusion method is used to evaluate sample antibacterial activity [12]. Before inserting the test organism, 10 ml of Mueller-Hilton agar medium was placed in sterile petri plates with a diameter of 60 mm. Mueller-Hilton agar plates were covered with sterile filter paper discs containing samples at 60, 80, and 100 g/ml concentrations. A filter paper disc containing 5 g of amoxicillin was used as a positive control. After incubating the plates at 37°C for 24 hours, the experiment was performed again. The inhibitory zone was measured in centimetres.

6.3. Antifungal activity measurement using the disc diffusion method

The antifungal activity of samples against test microorganisms was determined using the disc diffusion technique. The test organism was sown on petri dishes (60 mm) filled with Sabouraud's dextrose agar(SDA) with 0.3 ml of sterile filter paper discs (6 mm in diameter, Whatmann paper no. 3). At concentrations of 60, 80, and 100 g/ml, the 10 l of samples were impregnated into the sterile disc, correspondingly [13]. During a 24-hour incubation period at

37°C, the zones of growth inhibition surrounding the disc were assessed. However, fluconazole was used as a positive control.

7. Results

7.1. Anti-bacterial activity of sample

AgNPs provide intriguing prospects for the development of new biocompatible nanoscale components are being developed for novel antibacterial uses. By interfering with the nucleic acid chain of cell respiration (DNA or RNA), AgNPs cause damage to bacterial cell walls. Because of their high surface-to-volume ratio and unique chemical and physical features, Antibacterial agents against MDR bacteria have been created using AgNPs. As particle size drops, so does the surface area to volume ratio.

Table 1. In Vitro Antibacterial activity of samples.

Samples	***Concentrations (µg/ml)***	***Organisms/Zone of inhibition (mm)***					
		Pseudomonas aeruginosa	***Proteus vulgaris***	***Enterococcus faecalis***	***Streptococcus mutans***	***Enterococcus aeruginosa***	***Bacillus subtilis***
Samples	*60*	*2*	*3*	*0*	*3*	*0*	*0*
	80	*3*	*4*	*5*	*6*	*5*	*1*
	100	*5*	*6*	*7*	*8*	*7*	*3*
Standard (Std) *(Amoxicillin)*	*10 µl/disc*	*8*	*9*	*8*	*10*	*9*	*8*
Aqueous	*10 µl/disc*	*0*	*0*	*0*	*0*	*0*	*0*

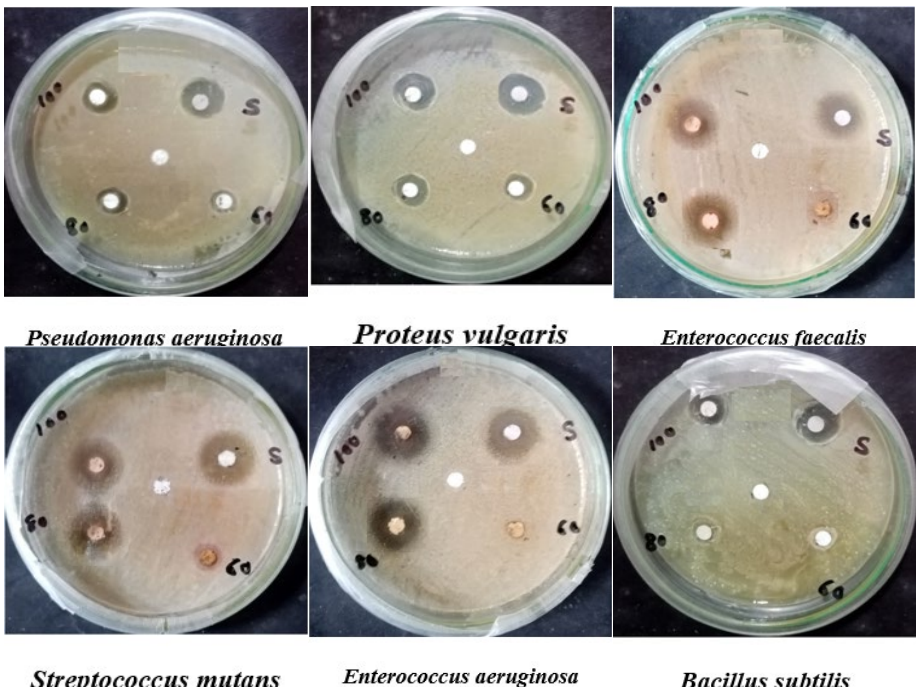

Fig. 7. Antibacterial activity of silver nanoparticles against six bacterias (1. Pseudomonas aeruginosa, 2. Proteus vulgaris, 3. Enterococcus faecalis, 4. Streptococcus Mutans, 5. Enterococcus aeruginosa, and 6. Bacillus subtilis).

The size and stability of AgNP particles suggested antibacterial action. The antibacterial action of NPs is influenced by their size and structure. Because smaller AgNPs have a wider binding surface, they are more effective against bacteria.

The death rate of six bacteria is shown in this table (Table-1): Pseudomonas aeruginosa, Proteus vulgaris, Enterococcus faecalis, Streptococcus mutans, Enterococcus aeruginosa, and Bacillus subtilis (Figure-8). The death rates of bacteria rose as the concentration of Ag nanoparticles was raised.

7.2. Anti-fungal activity of sample

Antifungal effects of nanoparticles against Aspergillus flavus and Candida vulgaris have been demonstrated (Figure-9). When combined with conventional antibiotics, AgNPs displayed improved stability and a more synergistic effect. The table (Table-2) depicts the fungal activity of Ag NPs.

Table 2. In Vitro Antifungal activity of samples.

Samples	***Concentrations (µg/ml)***	***Organisms/Zone of inhibition (mm)***	
		Samples	
		Aspergillus Flavus	***Candida Vulgaris***
Samples Methanol	*60*	*0*	*0*
	80	*4*	*1*
	100	*6*	*7*
Standard (Std) (Fluconazole)	*10 µl/disc*	*7*	*11*
Aqueous	*10 µl/disc*	*0*	*0*

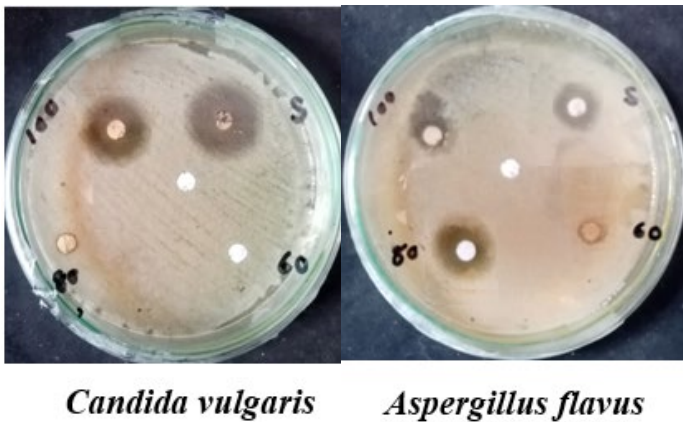

Fig. 8. Antifungal activity of silver nanoparticles against two fungi (Candida vulgaris and Aspergillus flavus).

8. Conclusion

The current work shows the bio reduction of silver nanoparticles using the helpful Crocus sativus petal extract by maximising the factors for a speedy and stable nanoparticle creation [14, 15]. The management of the nanoparticle generation process involved temperature, metal ion concentration, and incubation time [16]. The majority of the silver nanoparticles created are consequently spherical, according to SEM [17].

This environment friendly procedure is quick, simple, safe, and trustworthy because of its potent antimicrobial effect [18]. Silver nanoparticles are extremely powerful antibacterial agents against Pseudomonas aeruginosa, Proteus vulgaris, Enterococcus faecalis, Streptococcus mutans, Enterococcus aeruginosa, and Bacillus subtilis according to the antimicrobial research. As a result, there are many applications for silver nanoparticles in the fields of electrochemical and medical sensors [19, 20].

Acknowledgements

The corresponding author, A. Cathirin Preethi, acknowledges the National College Instrument facility, National College (Autonomous), Tiruchirappalli, Tamilnadu, India for "LAB FACILITY".

References

[1] Arumai Selvan D, Mahendiran D, Senthil Kumar R, et al., J Photochem Photobiol B. 2018;180:243-252; https://doi.org/10.1016/j.jphotobiol.2018.02.014

[2] Bagur H, Medidi RS , Somu P , et al. Mater Tech. 2020.

[3] Bredar, A. R. C., Chown, A. L., Burton, A. R. & Farnum, B. H.,ACS Appl. Energy Mater. 3, 66-98 (2020); https://doi.org/10.1021/acsaem.9b01965

[4] Darroudi, M., Ahmad, M. B., Abdullah, A. H., Ibrahim, N. A., Shameli, K. (2010); International Journal of Molecular Sciences, 11(10), 3898-3905; https://doi.org/10.3390/ijms11103898

[5] Du J, Hu Z, Yu Z, et al. Mater Sci Eng C. 2019;102:247-253; https://doi.org/10.1016/j.msec.2019.04.031

[6] Erci, F.; Cakir-Koc, R.; Isildak, I. Biotechnol. 2018, 46, 150- 158; https://doi.org/10.1080/21691401.2017.1415917

[7] Hemlata; Meena, P.R.; Singh, A.P.; Tejavath, K.K., ACS Omega 2020, 5, 5520-5528; https://doi.org/10.1021/acsomega.0c00155

[8] Hemashekhar Bagur, Raja Sekhar Medidi, Prathap Somu, P. W. Jayakumar Choudhury, Chetan Shekhar karua, Praveen Kumar Guttula, Govindappa Melappa & Chandrappa Chinna Poojari (2020), Mater Technol.

[9] Khalil, M.M.H.; Ismail, E.H.; El-Baghdady, K.Z.; Mohamed, D., Arab. J. Chem. 2014, 7, 1131-1139; https://doi.org/10.1016/j.arabjc.2013.04.007

[10] Kumari Jyoti, Devender Arora, Gusztáv Fekete, László Lendvai, Gábor Dogossy, Tej Singh (2020), Mater Technol.

[11] Lee SH, Jun BH. Int J Mol Sci. 2019;20(4):865; https://doi.org/10.3390/ijms20040865

[12] Mao QQ, Xu XY, Cao SY, et al., Foods. 2019;8(6):185; https://doi.org/10.3390/foods8060185

[13] Raja S, Ramesh V, Thivaharan V., Arabian J Chem. 2017;10:253261; https://doi.org/10.1016/j.arabjc.2015.06.023

[14] Rasheed T, Bilal M, Iqbal HM, et al., Colloids Surfaces B. 2017;158:408-415; https://doi.org/10.1016/j.colsurfb.2017.07.020

[15] Ravichandran V, Vasanthi S, Shalini S, et al. Results hys. 2019;15:102565; https://doi.org/10.1016/j.rinp.2019.102565

[16] Singh C, Kumar J, Kumar P, et al., Biotechnol Biotechnol Equip. 2019;33(1):359-371.

[17] Some, S.; Sen, I.K.; Mandal, A.; Aslan, T.; Ustun, Y.; Yilmaz, E.S.; Kati, A.; Demirbas, A.; Mandal, A.K.; Ocsoy, I., Mater. Res. Express 2019, 6, 012001; https://doi.org/10.1088/2053-1591/aae23e

[18] Veena S , Devasena T , Sathak SSM , et al., J Clust Sci. 2019;30:1591-1597;

https://doi.org/10.1007/s10876-019-01601-z
[19] Wang L, Xu H, Gu L, et al., Mater Technol. 2016;31(8):437-442;
https://doi.org/10.1080/10667857.2015.1105575
[20] Z. J. Jiang, C. Y. Liu, and Y. J. Li, Chemistry Letters, vol. 33, no. 5, pp. 498-499, 2004;
https://doi.org/10.1246/cl.2004.498